SF2A 2012
S. Boissier, P. de Laverny, N. Nardetto, R. Samadi, D. Valls-Gabaud and H. Wozniak (eds)

ON CLOSE-IN MAGNETIZED STAR-PLANET INTERACTIONS

A. Strugarek[1], A. S. Brun[1] and S. Matt[1]

Abstract. We present 2D magnetohydrodynamic simulations performed with the PLUTO code to model magnetized star-planet interactions. We study two simple scenarios of magnetized star-planet interactions: the *unipolar* and *dipolar* interactions. Despite the simplified hypotheses we consider in the model, the qualitative behavior of the interactions is very well recovered. These encouraging results promote further developments of the model to obtain predictions on the effect and the physical manifestation of magnetized star–close-in planet interactions.

Keywords: Stars: winds, Stars: planetary systems, Stars: coronae

1 Introduction

More than 830 exo-planets have been presently discovered[i]. The interactions between stars and their orbiting planets can be distinguished between *distant* gravitational (orbital motions, tides) and *direct* (hydro-)magnetic (stellar wind, radiation) interplays. Both interactions are likely to play a major role in determining habitability zones and in understanding planet dynamics. In addition, close-in giant planets may also impact the rotation and magnetic properties of their host stars (Donati et al. 2008; Bolmont et al. 2012). Finally, the magnetized interactions can yield enhanced localized emissions in the chromospheres of their host stars (Shkolnik et al. 2005). For these reasons, a better characterization of star-planet interactions (SPIs) would be highly valuable (Cuntz et al. 2000; Ip et al. 2004; Lanza 2009). In this paper, we focus on basic mechanisms that underly the *direct* magnetized SPIs.

Magnetized SPIs can be separated into two classes: the so-called *unipolar* (magnetized wind, unmagnetized planet) and *dipolar* (magnetized wind and planet) interactions (Zarka 2007). They were initially studied in the context of satellites orbiting in the magnetosphere of giant planets (Kivelson et al. 2004). The space plasma in the upper magnetospheres of planets and in stellar winds is characterized by a Knudsen number (mean free path over characteristic size of the system) much greater than unity. Hence, the fluid approximation does not hold because there is *a priori* no reason to consider that the plasma is locally thermally equilibrated: a kinetic modeling should be used to accurately represent it (Marsch 2006). Because of limited computation resources, the large scales involved in magnetized SPIs prevent us to use a global kinetic modeling. Magnetohydrodynamic (MHD) models (which are less expensive to simulate) have been therefore widely used instead. Such models are able to recover the global properties of stellar winds (Goldstein et al. 1995) and have been used either by fitting the equation of state to recover the exact solar wind (Wang & Sheeley 1990; Arge & Pizzo 2000), or by conducting parametric studies to derive general scaling laws (Washimi & Shibata 1993; Matt et al. 2012, and references therein). Cohen et al. (2011) simulated magnetized SPIs based on the former kind of modeling (using the so-called *WSA* model). In this paper, we base our study on the latter modeling approach, which will allow us to derive robust scaling laws for magnetized SPIs.

We develop in section 2 the method we use to study magnetized SPIs. Then, we apply our setup to the two basic cases of the unipolar and diploar interactions in section 3. We validate the modeling choices we made and are able to predict the action of a close-in planet on the stellar surface flows. Finally, we give the perspectives of this preliminary work in section 4.

[1] Laboratoire AIM Paris-Saclay, CEA/Irfu Université Paris-Diderot CNRS/INSU, F-91191 Gif-sur-Yvette.
[i] `http://exoplanet.eu`

2 Modeling magnetized star-planet interactions

The magnetized SPIs consists of the interaction between the magnetized wind of the host star and the magnetized or unmagnetized planet. Any modeling tackling these interactions have to treat plasmas associated with both the wind and the planet.

2.1 Wind modeling

Following numerous previous studies (*e.g.*, Ustyugova et al. 1999), we use standard MHD wind theory that characterizes magnetized steady-state flows anchored at the surface of a rotating star. The exact wind driving mechanism is still debated today, its details should not matter for the purpose of this paper. Hence we make the assumption that it is driven by the thermal pressure of the coronal plasma (which is a common basic assumption, *e.g.*, in the case of the solar wind).

We use the PLUTO code (Mignone et al. 2007) to calculate steady-state winds using the ideal compressible MHD equations (written here in their primitive formulation for simplicity)

$$\partial_t \rho + \boldsymbol{\nabla} \cdot (\rho \mathbf{v}) = 0\,, \tag{2.1}$$

$$\partial_t \mathbf{v} + \mathbf{v} \cdot \boldsymbol{\nabla} \mathbf{v} + \frac{1}{\rho} \boldsymbol{\nabla} P + \frac{1}{\rho} \mathbf{B} \times \boldsymbol{\nabla} \times \mathbf{B} = \mathbf{g}\,, \tag{2.2}$$

$$\partial_t P + \mathbf{v} \cdot \boldsymbol{\nabla} P + \rho c_s^2 \boldsymbol{\nabla} \cdot \mathbf{v} = 0\,, \tag{2.3}$$

$$\partial_t \mathbf{B} - \boldsymbol{\nabla} (\mathbf{v} \times \mathbf{B}) = 0\,, \tag{2.4}$$

where ρ is the density, $\mathbf{v}$ the velocity, P the gas pressure, $\mathbf{B}$ the magnetic field, $\mathbf{g}$ the gravitational acceleration, ∂_t the derivative with respect to time and $c_s = \sqrt{\gamma\, P/\rho}$ the sound speed (γ is the polytropic index of the plasma). We use an ideal gas equation of state.

We use the following options in PLUTO to run our simulations. A minmod limiter on all the variables and a *hll* (Harten, Lax, Van Leer) solver to compute the intercell fluxes. A second order Runge-Kutta scheme is used for the time evolution. The solenoidality of the magnetic field ($\boldsymbol{\nabla} \cdot \mathbf{B} = 0$) is ensured with a *constrained transport* (CT) method (*e.g.*, Gardiner & Stone 2005).

We initialize our simulation with the spherically symmetric hydrodynamic Parker solution (Parker 1958). We add a dipolar magnetic field characterized by the ratio $v_A/v_{\rm esc} = 0.32$ at the surface of the star ($v_A = B/\sqrt{4\pi\rho}$ is the Alfvèn speed and $v_{\rm esc} = \sqrt{2GM_\star/R_\star}$ is the escape speed). We developed special boundary conditions (Matt & Pudritz 2008; Zanni & Ferreira 2009) that ensure the conservation of the five quantities theoretically conserved along field lines that were identified by Lovelace et al. (1986) and Keppens & Goedbloed (2000). The parameters and characteristics of the simulated wind are given in table 1. The wind exhibits a large dead zone (closed field lines and very slow motions region) inside its alfvenic surface that extends up to $r \sim 7\,R_\star$ at the equator. We develop hereafter the methodology we use to simulate an orbiting planet.

Table 1. Parameters and deduced characteristics of the simulated stellar wind. The parameter $v_{\rm rot}/v_{\rm esc}$ sets the rotation rate of the star. The mass loss rate is normalized to $\rho_\star v_{\rm esc} R_\star^2$ and the angular momentum loss rate to $\rho_\star v_{\rm esc}^2 R_\star^3$. The ratio between opened and closed field lines is given by $\Psi_{\rm o}/\Psi_\star$ ($1-\Psi_{\rm o}/\Psi_\star$ gives the size of the dead zone, with $\Psi_{\rm o} \equiv \oint \mathbf{B}\cdot{\rm d}\mathbf{A}$). Finally, we give the typical poloidal velocity of the wind at ($r = 15\,R_\star, \theta = 45^\circ$).

Parameters	γ	$c_{\rm s}/v_{\rm esc}$	$v_{\rm rot}/v_{\rm esc}$	$v_{\rm A}/v_{\rm esc}$
	1.05	0.2220	0.00303	0.3183
Characteristics	$\dot{m}$	$\Psi_{\rm o}/\Psi_\star$	$\dot{j}$	$v_{\rm p}/v_{\rm esc}$ ($15r_*$, 45°)
	$6.48\ 10^{-4}$	0.251	$7.12\ 10^{-4}$	0.250

2.2 Planet modeling

We introduce a planet as a boundary condition inside the computational domain. We choose to study only close-in planets in this paper, *i.e.* planets which are *inside* the dead-zone of the stellar wind. Hence, we introduce a very close planet at $r_{\rm orb} = 2.5\,R_\star$. The type of interaction between the two bodies is determined by the topology of the planetary magnetic field. We choose a heavy Jupiter-like planet such that $r_P = 0.1\,R_\star$ ($R_J \sim 0.1\,R_\odot$) and $m_p = 0.01\,M_\star$ ($M_J = 0.001\,M_\odot$). We design a stretched grid such that the typical resolution is of the order

of $r_P/32$ at the planet surface and of $R_\star/64$ at the stellar surface. We ensured the numerical convergence of our results when increasing the resolution by a factor two.

The initialization of the planet in the steady-state wind creates a transient evolution that is rapidly forgotten. Because we use an idealized axisymmetric configuration (the so-called 2.5D approximation, *i.e.*, we study the 3D fields only on an axisymmetric poloidal plane), the planet we simulate has the shape of a torus circling the star, rather than a sphere. As a consequence, the orbital motion does not introduce any time-variability in the orbital direction and a new steady-state can be obtained. Even if this situation is far from reality, it constitutes a first step towards the realistic modeling of magnetized SPIs (see perspectives in section 4).

3 Basic interactions

As mentioned in the introduction, the magnetized SPIs can be decomposed into *unipolar* and *dipolar* interactions (Zarka 2007). We successively simulate the two situations in the following, which are very well recovered by our model.

– **Unipolar interaction** – We introduce a unmagnetized rotating planet in the dead zone of the simulated wind (section 2.1). This system is equivalent to the well known interaction of Io in the magnetosphere of Jupiter. The unmagnetized planet drags the poloidal magnetic field lines and current sheets establish along the poloidal field lines connecting the planet to the host star (Goldreich & Lynden-Bell 1969). We indeed observe a current loop in figure 1(a) that connect the planet and the star together (the black arrows represent the current density $\mathbf{J} = \boldsymbol{\nabla} \times \mathbf{B}$). An azimuthal component of the magnetic field (B_φ) is also naturally created through an effective 'Omega'-effect generated by the orbital motion of the planet. A steady state situation is achieved when the numerical diffusion of the magnetic field in the azimuthal direction is balanced by the continuous twisting action of the differential rotation between the star and planet orbit. A steady state return flow from the planet to the star is then associated with the magnetic flux-tube. The magnetic connection between the star and the planet implies the existence of a torque between the two objects. The planet orbits at the keplerian velocity (such that its orbital motion compensates the stellar gravitational pull), hence it rotates much faster than the stellar surface (*i.e.*, the co-rotation radius is larger than the orbital radius of the planet). The planet exerts consequently a torque localized in latitude which is approximately 4 times larger (and of opposite sign) than the overall torque exerted by the stellar wind when no planet is taken into account. The exact value of the torque is likely to depend on both *(i)* the fact that we are considering a 2D setup and *(ii)* the amount of numerical diffusivity.

– **Dipolar interaction** – We also perform the exact same simulation with a *magnetized* planet. We choose a dipolar planetary magnetic field anti-aligned with the initial stellar dipole (we choose its original amplitude such that the initial planetary magnetosphere is of the order of $2\,r_p$). As a consequence, the closed magnetic field lines of the wind naturally connect at the poles of the planet, and magnetic reconnection occur at the equator where the magnetic field lines of the wind and of the planet are anti-aligned. We also note here that the planetary field only resembles a dipole in the poloidal plane but was slightly modified to preserve $\boldsymbol{\nabla} \cdot \mathbf{B} = 0$ in an axisymmetric geometry. We display in figure 1(b) the interaction between the magnetized planet and the stellar wind.

Reconnections of the magnetic field lines occur at the equator and are labeled by the dashed white line. We see that the field lines connect together the planet and the stellar surfaces (dashed red line). Because these field lines are close to the closed-opened field lines boundary, they tend to be advected by the stellar wind and are stretched away from the planet (yellow dashed line). Reconnection then occur again and the magnetic field lines close in the magneto-tail of the planetary magnetosphere (black dashed line). This process is very similar to the basic reconnection mechanism developed to explain the structure of the magnetosphere of the planets of the solar system (Gombosi 1998).

We recall here that these numerical experiments are done in the framework of ideal MHD. Hence, any reconnection occurring in the simulations is controlled by the effective diffusion introduced by the numerical techniques we use. In order to quantitatively characterize the reconnection process we observe, a better control of the ohmic diffusion is mandatory and will be adressed in future work.

Finally, the magnetic connection between the two objects is stronger than in the unipolar case and the torque exerted by the planet on the stellar surface is roughly twenty times larger (and of opposite magnitude) than the torque exerted by the stellar wind.

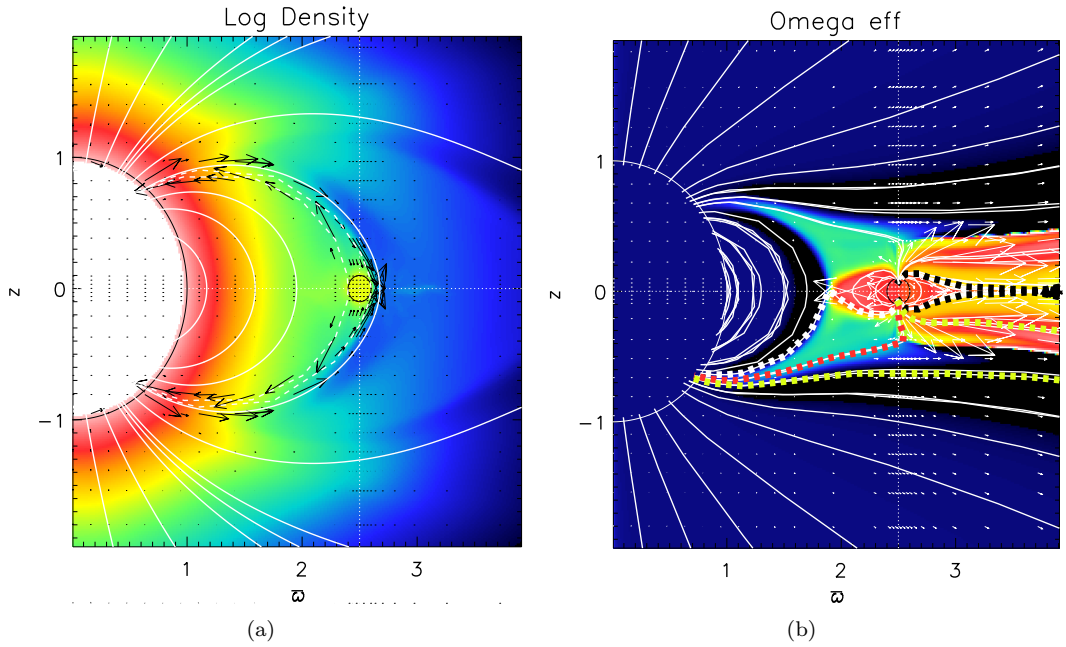

Fig. 1. Left: Simulation of the unipolar interaction. The color map represents the logarithm of density (blue/black is low density, red/white high density) and the black arrows are the current density **J**. **Right:** Simulation of the dipolar interaction. The colormap represent the effective rotation rate $\Omega_{\rm eff} = \frac{1}{\varpi}\left(v_\varphi - \frac{\mathbf{v}_p\cdot\mathbf{B}_p}{B_p^2}B_\varphi\right)$, where (ϖ, φ, z) are the cylindrical coordinates and the subscript p denotes the poloidal (ϖ, z) component of the field. The rotation rate of the star is blue. The white arrows are the velocity field.

4 Conclusions and perspectives

In this paper, we demonstrated that ideal MHD simulations in 2D axisymmetric geometry could well capture the basic magnetized SPIs involving a close-in giant planet orbiting inside the alfvenic surface of its host star. We tested both the unipolar (unmagnetized planet) and dipole (magnetized planet) interactions and showed that the former were likely to exert a greater torque on the stellar surface. Because the planet orbital motion and the rotation rate of the star are fixed, the applied torque does not modify the surface rotation nor the planet orbit. Fixing them is legitimate here since approximately 10^{14} orbits would be required to change the orbital radius by $0.1\,R_\star$ in the unipolar case (based on the observed torque in the simulations). This picture may drastically change when varying the wind and planet parameters.

We established a modeling framework that will allow us to develop a complete numerical analysis of magnetized SPIs. The obvious next step consist naturally in simulating the star-planet pairs in 3D in order to let the interaction develop in the correct geometry. Then, we will be able to explore the various interaction regimes depending on the magnetic topologies and time-variability of the stellar and planetary fields, and on the position of the planetary orbit in the stellar wind. Finally, we also intend to develop tools to determine the expected level of emissions resulting from the magnetized SPIs (*e.g.*, see Vidotto et al. 2012). This work will lead to reliable scaling laws on the effect of magnetized SPIs that will be useful to explain and guide exoplanet observations, but also to test fundamental ideas explaining the physical processes underlying these interactions.

The authors thank N. Bessolaz, R. Pinto and C. Zanni for very helpful discussions at the origin of this work.

References

Arge, C. N. & Pizzo, V. J. 2000, JGR, 105, 10465
Bolmont, E., Raymond, S. N., Leconte, J., & Matt, S. P. 2012, A&A, 544, 124
Cohen, O., Kashyap, V. L., Drake, J. J., et al. 2011, ApJ, 733, 67
Cuntz, M., Saar, S. H., & Musielak, Z. E. 2000, ApJ, 533, L151

Donati, J.-F., Moutou, C., Fares, R., et al. 2008, MNRAS, 385, 1179
Gardiner, T. A. & Stone, J. M. 2005, JCP, 205, 509
Goldreich, P. & Lynden-Bell, D. 1969, ApJ, 156, 59
Goldstein, M. L., Roberts, D. A., & Matthaeus, W. H. 1995, Annual Review of A&A, 33, 283
Gombosi, T. I. 1998, Physics of the space environment (Physics of the space environment / Tamas I. Gombosi. Cambridge ; New York : Cambridge University Press)
Ip, W.-H., Kopp, A., & Hu, J.-H. 2004, ApJ, 602, L53
Keppens, R. & Goedbloed, J. P. 2000, ApJ, 530, 1036
Kivelson, M. G., Bagenal, F., Kurth, W. S., et al. 2004, In: Jupiter. The planet, 513
Lanza, A. F. 2009, Astronomy and Astrophysics, 505, 339
Lovelace, R. V. E., Mehanian, C., Mobarry, C. M., & Sulkanen, M. E. 1986, ApJ Supp. Series, 62, 1
Marsch, E. 2006, Living Review on Solar Physics, 3, 1
Matt, S. & Pudritz, R. E. 2008, ApJ, 678, 1109
Matt, S. P., MacGregor, K. B., Pinsonneault, M. H., & Greene, T. P. 2012, ApJ Letters, 754, L26
Mignone, A., Bodo, G., Massaglia, S., et al. 2007, ApJ Supp. Series, 170, 228
Parker, E. N. 1958, ApJ, 128, 664
Shkolnik, E. L., Walker, G. A. H., Bohlender, D. A., Gu, P. G., & Kürster, M. 2005, ApJ, 622, 1075
Ustyugova, G. V., Koldoba, A. V., Romanova, M. M., Chechetkin, V. M., & Lovelace, R. V. E. 1999, ApJ, 516, 221
Vidotto, A. A., Fares, R., Jardine, M., et al. 2012, arXiv: 1204.3843
Wang, Y.-M. & Sheeley, N. R. J. 1990, ApJ, 355, 726
Washimi, H. & Shibata, S. 1993, MNRAS, 262, 936
Zanni, C. & Ferreira, J. 2009, A&A, 508, 1117
Zarka, P. 2007, Planetary and Space Science, 55, 598